EXPERIMENTS ON ULTRASHORT, ULTRAINTENSE LASER INTERACTION WITH THIN FOILS

M. Galimberti, A. Giulietti, D. Giulietti[@], L.A. Gizzi #,
Intense Laser Irradiation Laboratory - IFAM, Area della Ricerca CNR, Via Alfieri, 1 - 56010, Ghezzano, Pisa, Italy
[@]*also at* Dipartimento di Fisica, Universit di Pisa, and INFM, Pisa Italy

F. Balcou, A. Rousse, J. Ph. Rousseau
Laboratoire d Optique Appliqu e - ENSTA, 91120, Palaieseau cedex, France

We have performed a series of experiments at the Laboratoire d'Optique Appliqu e in which intense femtosecond pulses of a Ti:Sapphire laser were focused on a thin plastic foil at an intensity up to 10^{20}W/cm^2. In these experiments the laser field at the focal position is confined in a wave-packet as short as 10 m (approximately 10 optical cycles) and less than 10 m in width. In such conditions electrons of the target experience electric fields exceeding by orders of magnitude the atomic fields.

Optical, X-ray and gamma-ray techniques implemented to investigate this interaction regime show that the dynamics of the interaction depends strongly upon the laser pre-pulse features on a high dynamic range in both the time and the intensity domain. If the intensity of the pre-pulse is below the plasma formation threshold, the main femtosecond pulse interacts directly with a thin, dense, sharply-bounded layer. In contrast, in the presence of an intense pre-pulse, premature explosion of the foil occurs and the femtosecond pulse propagates through a pre-formed plasma. Novel observations and measurements performed recently are presented and discussed here.

1. INTRODUCTION

High-power, ultra-short lasers based upon chirped pulse amplification (CPA) have now been available for several years[1] and different experimental schemes of laser interaction with matter have been conceived and explored. In principle, the lack of hydrodynamic expansion during the pulse duration (<< 1ps) makes it possible to achieve a completely unexplored domain of extremely high fields in solid-density ionised matter. However, "real world" CPA lasers are usually characterised by low level pre-emission (pre-pulse) originating either from amplified spontaneous emission (ASE) or from a leakage of the chirped pulse through the compression stage. If the intensity on target due to this pre-pulse is higher than the threshold intensity for plasma formation, a precursor plasma *(pre-plasma)* is formed which prevents the main femtosecond pulse from interacting directly with the solid. A schematic view of a CPA pulse structure on a high dynamic range scale is shown in Fig.1.

These features of a CPA laser system are usually summarised by giving the *contrast ratio*, i.e. the ratio of the CPA peak power to the power taken at a given time before the peak. Typical contrast ratios for presently available CPA systems are hardly greater that 10^7. With the peak intensity on target achievable today, that is up to 10^{20} W/cm^2, the pre-pulse intensity on target on a nanosecond time-scale can be greater than 10^{13}W/cm^2, i.e., above the plasma formation threshold of most solid targets. One way of increasing the contrast ratio is based upon frequency doubling of the pulse. However, the improvement in this case is often limited by the contrast of the oscillator pulse itself which typically is not better than 10^4-10^5. Recently a more systematic approach has been proposed[2] based upon the use of a saturable absorber to "clean" the unstretched, pre-amplified oscillator pulse.

In the general case of CPA laser-solid interactions however, we can expect that the CPA pulse interacts with a pre-formed plasma whose scale-length, density and temperature will depend upon the time at which

invited talk at the International Conference on LASERS 2000, Dec. 4-8, 2000, Albuquerque, NM, USA

premature plasma formation has occurred. Therefore, the dominant physical processes in the interaction depend on both target properties and laser features on a large dynamic range in time and intensity.

2. OUR EXPERIMENTAL TECHNIQUE

We tackle the problem of the control of the interaction regime by using well-characterised thin plastic (FORMVAR) foils as targets. In fact, thin foils have been found to exhibit high laser damage thresholds and, due to their optical transparency, volume laser propagation prior to breakdown is enabled. Also, these targets are transparent to forward emission of radiation (ω, X, γ) and particles (e^-, e^+ p, n etc) generated during the interaction at high intensity. In addition, due to their planar symmetry, optical diagnostics of transmission and reflection can provide valuable information on energy balance issues. On the other hand the exploding foil technique is well established as a highly reliable plasma pre-forming method. Smooth long-scale-length plasmas can be easily generated and characterised[3] and peak plasma densities above the critical density can be easily achieved.

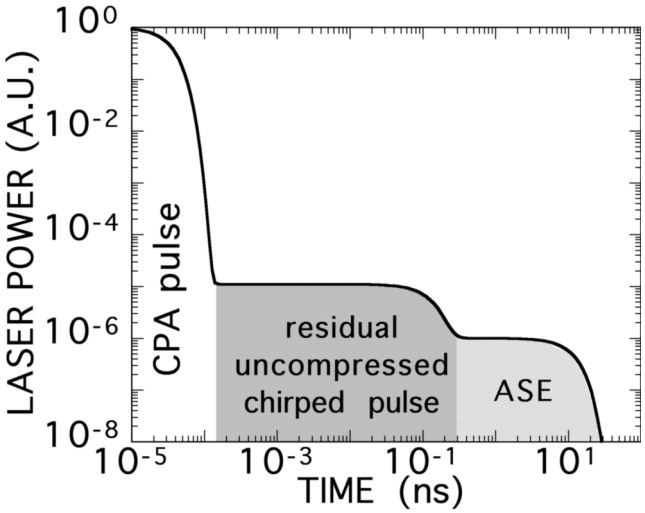

Fig.1 CPA lasers are usually characterised by a low level pre-emission (pre-pulse) originating either from the amplified spontaneous emission (ASE) or from a leakage of the chirped pulse through the compression stage. The intensity on target due to this pre-pulse can be higher than the threshold intensity for plasma formation, giving rise to a precursor plasma *(pre-plasma)* which prevents the femtosecond pulse from interacting directly with the solid.

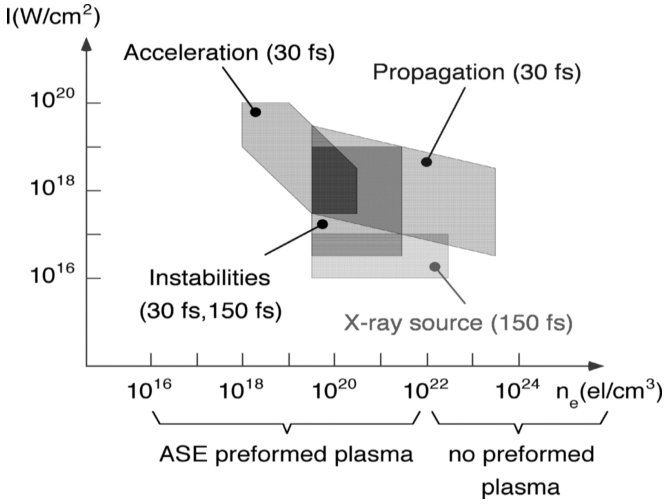

Fig.2 Regions of the laser intensity-plasma density space explored experimentally in ultra-short CPA interaction experiments performed at the Laboratoire d'Optique Appliqu e using thin foil targets. Here the vertical axis represents the peak laser intensity available in the laser focal plane while the horizontal axis represents the typical plasma electron density that dominates the interaction, depending on the contrast ratio of the laser.

Plasma formation thresholds of these foil targets were investigated experimentally at the Intense Laser Irradiation Laboratory at IFAM-CNR by using a Nd:YAG laser with well-characterised spatial and temporal profiles[4]. Experimental data are in agreement with a simple 2D analytical model based upon local transmissivity-ionisation-reflectivity which accounts for the actual laser intensity distribution on targets. These measurements show that, depending on the angle of incidence and polarisation, the plasma formation threshold for 40 ps pulses can be as high as 10^{13} W/cm^2 while for nanosecond pulses is decreases by a factor of 10 or more.

With this kind of targets we have performed several experiments at the Laboratoire d'Optique Appliqu e under the EU programme of Access to Large Laser Facilities. We used either the 150 fs laser system or the newly developed 30 fs system, now capable of delivering up to 1J on target. In this way we were able to access several regimes of interaction which can be schematically identified by four regions in the intensity-density space as depicted in Fig.2. Here the vertical axis represents the peak laser intensity available in the

laser focal spot while the horizontal axis represents the typical plasma electron density that dominates the interaction, depending on the contrast ratio of the laser.

3. PREVIOUS EXPERIMENTS

3.1 Steep plasmas and X-ray emission

In the case of the region referred to as the *X-ray source*, the investigation was carried out using a 150 fs laser pulse focused on a 0.8 m thick plastic foil at an intensity of 5 x 10^{17} W/cm^2. In this case the ASE intensity on target was below the plasma formation threshold; the plasma density scale-length was set by the ps pedestal and was of the order of the laser wavelength or less. Important physical issues in this case are energy absorption and X-ray generation. A strong evidence of the interaction with a steep density gradient was found studying the X-ray emission as a function of the polarisation of the incident laser light that was varied continuously from *S* to *P,* as shown in Fig.3. As we can see, an increase of more than two orders of magnitude in the intensity of the X-ray emission was found when going from *S* to *P*. This is explained[5] in terms of resonance absorption at the critical density layer.

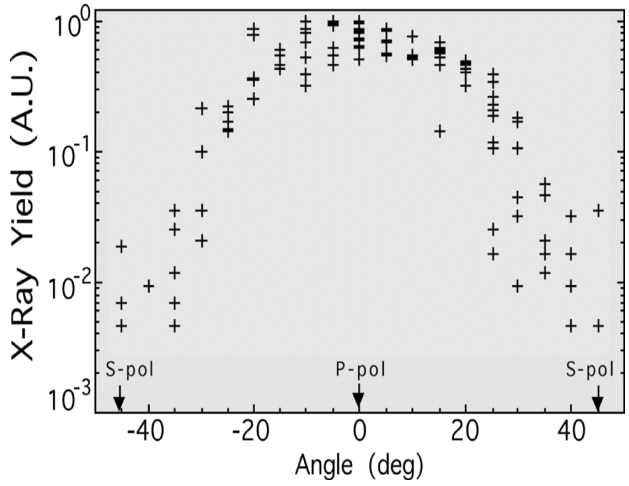

Fig.3 X-ray emission as a function of the polarisation of the incident laser light in the interaction of a 150 fs laser pulse with a 0.8 m thick plastic foil at an intensity of 5 x 10^{17} W/cm^2. The strong polarisation dependence is an evidence of the presence of a steep plasma density that could be achieved thanks to the low level of ASE on target.

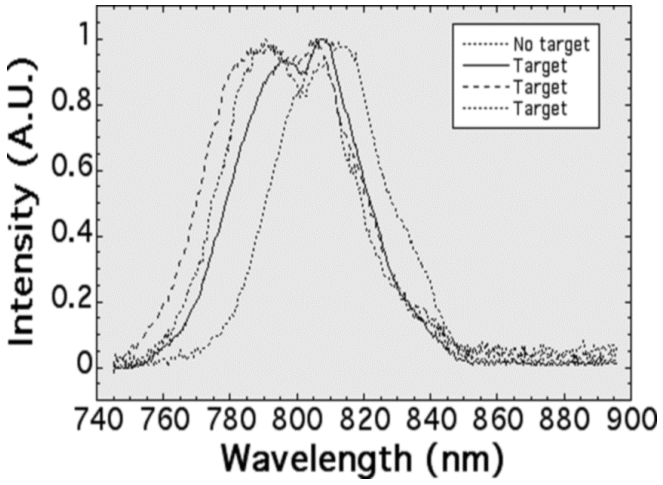

Fig.4 Spectra of laser light transmitted through a 0.1 m thick plastic foil showing a blue-shift induced by volume ionisation in the target. The laser pulse-length was 30 fs and the intensity on target was 4x10^{17} W/cm^2. This blue-shift is explained in terms of self-phase modulation in a rapidly ionising plasma.

3.2 Anomalous propagation

Unexpected propagation features were found for shorter pulses (see the region of Fig.2 referred to as the *propagation* region). As in the experiment above, also in this case we were able to achieve the conditions of no premature plasma formation, so that the 30 fs pulse could reach the unexploded foil at an intensity up to 3x10^{18} W/cm^2. We found that the spectrum of the laser radiation transmitted through the foil was blue-shifted with the blue shift increasing with the laser intensity. Fig. 4 shows three different spectra of the transmitted light compared with the spectrum of the unperturbed incident laser light. This blue shift is explained [6] in terms of self-phase modulation in a rapidly ionising plasma. Assuming a change in the refractive index of the medium equal to -1 (from cold matter to plasma) over a length of 0.1 m, equal to the target thickness, the shift of 13nm measured at 5x10^{16} W/cm^2 gives a ionisation time of 20fs. At 4x10^{17} W/cm^2 the average blue-shift becomes 20 nm which corresponds to an ionisation time of 13 fs.

These results were also correlated with measurements of the fraction of energy transmitted through the target. It was found that the transmissivity of the target increased with the intensity giving almost complete transparency at $3x10^{18}$ W/cm^2. A possible mechanism for this anomalous over-dense laminar plasma transparency has been proposed [7] which is based upon an extraordinary propagation in a magnetised plasma.

In that experiment we also carried out preliminary measurements of hard X-ray emission which showed that a component of very fast electrons is generated during the interaction process. In fact, the X-ray radiation emitted directly from the target using a collimator was compared with the non-collimated background (see Fig.5) in a single photon detection regime. We found that, on average, background photons had twice the energy of photons emitted by the target directly. In other words, high-energy photons are the result of a secondary process that is most likely due to very fast electrons escaping from the target and generating bremsstrahlung radiation when interacting with the walls of the interaction chamber.

3.3 Premature plasma formation

If laser intensity is further increased, eventually we end up in a regime in which ASE on target is higher than the plasma formation threshold. A typical exploding-foil-like plasma is generated whose peak density can be varied changing the thickness of the target. This plasma can expand for nanoseconds before the arrival of the main CPA pulse. Therefore, at the time of interaction, a large scale-length plasma has developed which can give rise to a variety of interaction processes. The presence of a pre-formed plasma can be inferred by the onset of laser-driven plasma instabilities [8]. For example, emission [9] of radiation at $3\omega_L/2$, (ω_L is the fundamental laser frequency) is an evidence of the so-called two-plasmon decay instability which takes place at around a quarter of the critical density.

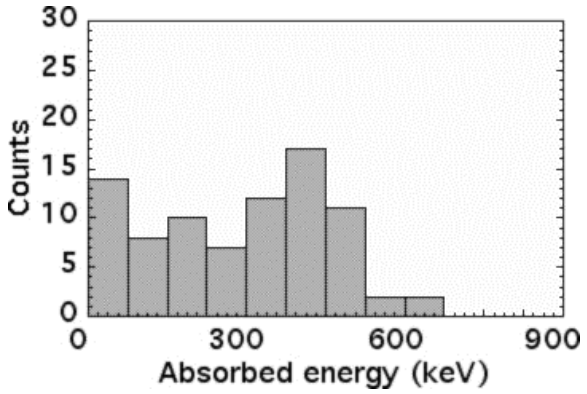

Fig.5 Hard X-rays emitted during the interaction of a 30 fs pulse with a thin plastic foil at an intensity of $3x10^{18}$ W/cm^2. The detector, a NaI(Tl) crystal coupled with a photo-multiplier, working in a single-photon regime, measured the energy of photons emitted by bremsstrahlung of fast electrons.

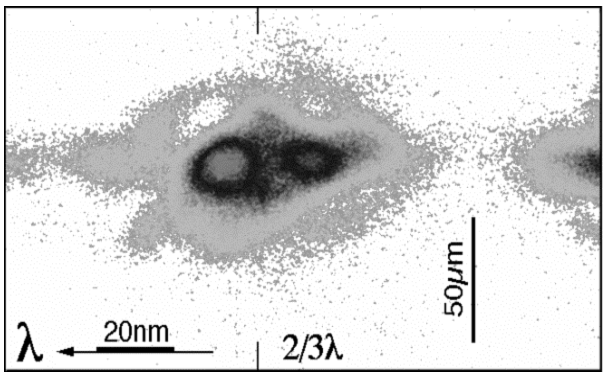

Fig.6 $3\omega_L/2$ radiation emitted in the specular direction in the interaction of a 30 fs laser pulse with a 1 m thick plastic foil. The emission originates from the two-plasmon decay instability occurring in the pre-plasma generated by the laser pre-pulse (ASE).

We use optical spectroscopy of light scattered, for example, in the direction of specular reflection to look for evidence of instabilities. An example of 3/2 ω_L spectrum found in conditions of ASE on target above plasma formation threshold is shown in Fig.6. Here the interaction region on target was imaged on the input slit of the spectrometer to achieve simultaneously spectral resolution (horizontal) and spatial resolution in the vertical direction. The 3/2 ω_L emission is very broad with strong modulations both in the spectral and spatial direction. Besides the information on the dynamics of the instability, spectra like this allow the regime of interaction to be easily monitored in order to identify the effect of laser pre-pulse.

3.4 Interactions with pre-formed plasmas: laser wakefield acceleration experiment

In some circumstances the presence of a pre-pulse can be exploited to generate controlled pre-formed plasma conditions. In the most recent experiment at LOA, we have demonstrated the possibility of tuning laser-foil interaction parameters for efficient acceleration of electrons by laser wakefield (LWA)[10]. Among a number of different schemes considered so far, the laser wake-field acceleration has become one of the most promising due to the recent availability of very powerful laser pulses lasting few optical cycles. The simplest model of such a mechanism is based on the interaction of a pulse of duration τ with a uniform plasma whose density n_e allows resonant excitation of electron waves of period $T \sim 2\tau$. More accurate calculations[11] show that optimum conditions also depend on the pulse temporal shaping. Assuming an acceleration length dominated by diffraction (Rayleigh length) one finds that the maximum energy gain of a particle in the field of a Gaussian laser beam is independent from the laser spot size. Higher gains can be achieved if the acceleration length exceeds the Rayleigh length, due to non-linear and/or hydrodynamic phenomena like beam trapping, self-channelling, or existing pre-formed channels. In these cases another limit to the acceleration length is given by the de-phasing length, which is of the order of λ_p^3/λ_o^2 , where λ_p and λ_0 are the electron plasma and laser wavelength, respectively.

A crucial issue to obtain high LWA gain is the production of a suitable plasma for an efficient interaction with the ultra-short laser pulse. The laser-driven exploding foil technique can provide plasmas of long scale-length with rather controllable density profiles. Such plasmas can also be simulated in advance using hydrodynamic numerical codes and can be characterised experimentally in detail. Foil thickness and material, together with the laser parameters are the essential input parameters in order to obtain a plasma of the required peak density and scale-length. For the 30-fs (Gaussian in time) Ti-Sapphire LOA laser pulse that we used in our experiment, the optimum plasma density is approximately 2×10^{18} cm^{-3}.

The basic idea of the experiment was therefore to try to profit of the nanosecond pedestal to pre-form a plasma having a density of the order of the one estimated above over a suitable length. After a careful characterisation of the pre-pulse of the LOA laser, we found that the contrast ratio, i.e. the ratio between the power delivered in the fs pulse and the one delivered by the 10 ns long ASE, was $\sim 10^{6}$. Therefore the ASE intensity on target was 10^{14} W/cm^2. 2-D hydro-code simulation[12] showed that with this ASE intensity, a long scale-length plasma with a peak density of 2×10^{18} cm^{-3} can be achieved with a $\sim$1 m thick plastic foil. In addition, hydrodynamic simulations also predict the presence of a weak density depression (channel) on the propagation axis. Therefore we were able to achieve a condition in which the main CPA pulse propagates in a plasma with a longitudinal scale-length of $\sim$200 m with an intensity of 10^{20} W/cm^2.

A schematic set up of this experiment is shown in Fig.7. The main diagnostics consisted of detectors for γ-ray emission from bremsstrahlung of accelerated electrons. When dealing with large fluxes of pulsed γ-ray radiation, as in our case, spectral and angular information can be obtained by using several γ-ray detectors whose sensitivities are optimised for different photon energies. We used four 24.5-mm diameter scintillators of 12.5-mm, 25.4-mm, and 50.8-mm thickness respectively, coupled to photomultipliers (PMs). The detectors were shielded by the heavy background radiation by means of lead bricks, while the line of sight was attenuated with layers of lead sufficiently thick to keep the PM signal below saturation.

The detectors were placed 5 meters away from the target and could be moved around the chamber to perform angular distribution measurements. The response of our detectors is characterised by a pulse with a rise time of the order of a few ns, set by the photomultiplier tube, and by a fall time of 230 ns, which is the decay time of the scintillator. The height of the pulse is a measure of the energy released by one or more photons in the scintillation crystal. The detectors had been calibrated, in the single photon regime, using emission lines from radioactive sources including the 511 keV and 1274 keV lines from ^{22}Na source and 898 keV and 1836 keV lines from a ^{88}Y source. According to this calibration the pulse height was found to be linearly dependent on the photon energy in this range. The working principle of our detectors is shown in

detail in Fig.8a. High-energy electrons generated during the interaction impinge on a thick layer of material (the walls of the interaction chamber) which acts as a bremsstrahlung converter. Bremsstrahlung γ-ray photons are emitted in a cone of aperture $\alpha \sim 1/\gamma$ where γ is the relativistic factor. Provided that the electron energy is sufficiently high (>> 1MeV), the original electron angular distribution is preserved and can be retrieved from the photon angular distribution. Fig.8b shows the angular spread of bremsstrahlung photons generated by the interaction of fast electrons calculated using Montecarlo (GEANT [13]) simulations [14] for our experimental set-up. The spectral properties of electrons can be obtained by comparison of measured signals with the predictions of Montecarlo simulations (GEANT). This technique works best for very large electron energies where traditional electron spectrometers based upon magnetic field become heavy and bulky.

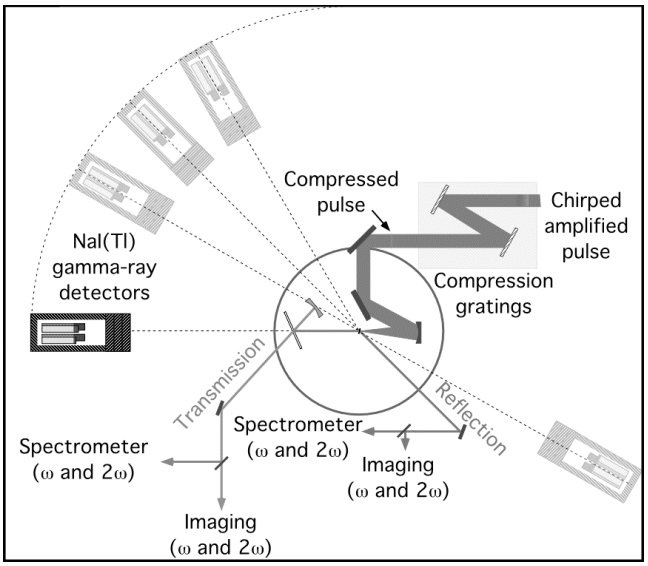

Fig.7 Experimental set up for the study of wakefield acceleration of electrons in the interaction of a ultra-intense CPA pulse with a pre-formed plasma. The plasma was produced by explosion of a 1 m thick plastic foil by the laser pre-pulse (ASE). Also shown are the main diagnostics for optical and γ-ray measurements.

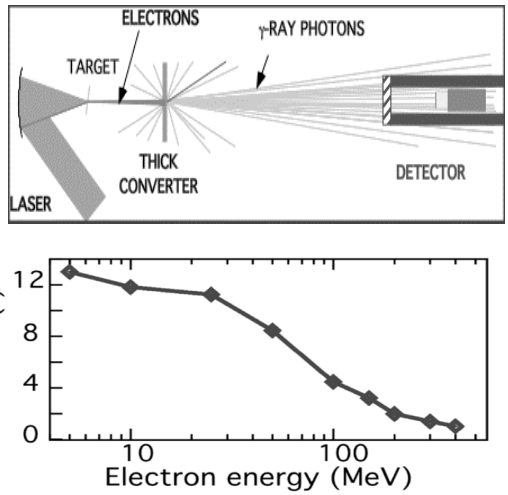

Fig.8a (top) Detector arrangement for the study of fast electrons produced in high intensity laser-plasma interactions. Bremsstrahlung emission of high-energy electrons (>MeV) is confined in a cone of aperture $\alpha \sim 1/\gamma$. **Fig.8b** (bottom) Angular spread of bremsstrahlung photons generated by the interaction of fast electrons calculated using Montecarlo (GEANT) simulations for our experimental set up. The higher the electron energy, the smaller is the angular spread of γ-ray photons.

We observe here that due to the unexpected high γ-ray flux on detectors, very thick layers of lead had to be used to reduce the PM signals down to a working regime. In this configuration lead acts as a simple, energy independent attenuator which reduces the signal by approximately one order of magnitude every 5cm of lead (exponential law) for all energies. Therefore additional data is needed to obtain spectral properties of these γ-rays. However, Montecarlo simulations compared to our γ-ray measurements strongly suggest that a population of fast electron with energies of many tens of MeV is generated.

As in the case of Fig.5, our signal consists of a collimated component originating from primary electrons and a diffused component due to secondary scattering processes. The diffused component can be separated from the collimated one by taking into account the measured dependence of the γ-ray signal as a function of the thickness of lead. Fig.9 shows the dependence of the bremsstrahlung γ-ray signal, for all four detectors, as a function of the thickness of the attenuator. The diffused component of γ-ray photons is obtained by fitting of the data with the function $S(x) = S_c A^{-x/x_0} + B$, where S_c is the collimated component, A is the attenuation coefficient for a 5 cm thick attenuator, x_0 is the lead thickness and B is the diffused component. The result of the fit is shown by the solid curves in Fig.9. According to this result, the signal after 15 cm of

lead attenuator is mostly due to the diffused component, while for smaller thickness the collimated γ-ray component accounts for most of the signal.

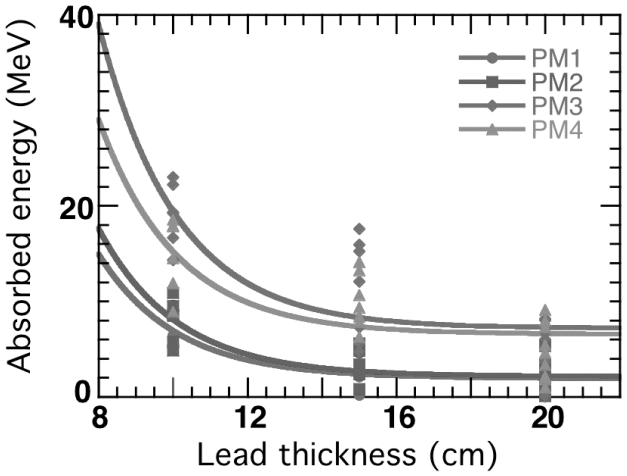

Fig.9 Dependence of the bremsstrahlung γ-ray signal as a function of the thickness of the lead attenuator. The diffused component of γ-ray photons is obtained by fitting of the data with a suitable function (see text).

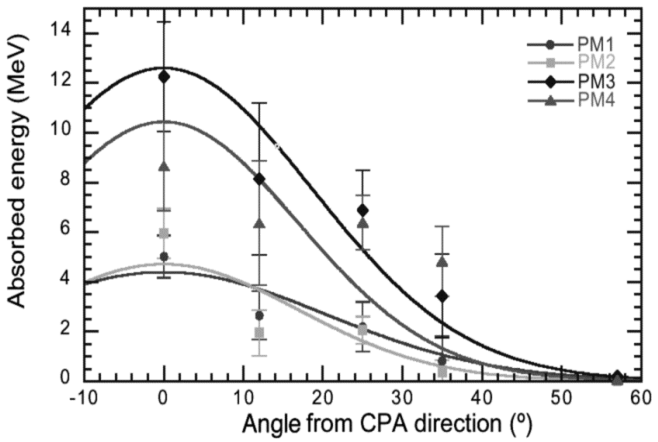

Fig.10 Angular distribution of bremsstrahlung γ-ray photons detected by the four NaI detectors assembled together. Also shown are the fitting curves which yield an aperture of the angular distribution of $\Theta_{FWHM} = 42.5 – 0.5$ deg.

The angular distribution of the collimated component was then measured by moving the detector assembly around the target chamber at a distance of 5m. Data were taken with different attenuator thicknesses depending on the signal strength. The result is summarised in the plot of Fig.10 were the signal of all the four detectors is shown. The data were fitted with a curve of the type $S_c = A \exp(8 \ln 2 \cos\theta / \Theta^2_{FWHM})$ which yields an aperture $\Theta_{FWHM} = 42.5 – 0.5$ deg.

We also studied experimentally the dependence of the γ-ray signal upon the thickness of the exploding foil target. As discussed above, the configuration we have chosen to optimise acceleration conditions was based upon a 1.0 m thick target. Indeed our measurements show that when thinner targets (0.1 m) are used (resulting in a lower peak density plasma) the γ-ray signal shows a reduction of at least two orders of magnitude when compared to the case of interaction with a 1.0 m thick target. Furthermore, a dramatic decrease of the γ-ray signal is observed when the 1.0 m foil is moved out of the best focus of the laser focusing optics. All these data, combined with the information acquired from simultaneous optical measurements[15] consistently show that conditions for resonant wake-field acceleration were achieved in our experiment.

CONCLUSIONS

The experiments discussed here show that dramatically different laser-plasma interaction regimes can take place in ultra-intense laser-solid interactions depending on the laser pulse features on the ns and ps time-scale. Thin plastic foils have been successfully used to perform interaction experiments with ultra-short, ultra-intense CPA laser pulses under controllable conditions. Strong, polarisation dependent laser-plasma coupling in steep density gradients has been studied at intensities up to 5×10^{17} W/cm^2. Laser-solid interactions with consequent ultra-fast ionisation of matter has been achieved at intensities up to 3×10^{18} W/cm^2. Finally, it was shown that, in ASE-dominated, single beam CPA interactions with thin foils up to 10^{20} W/cm^2, controlled pre-formed plasma conditions can be achieved which provide suitable conditions for the acceleration of electrons in the resonant wakefield scheme.

ACKNOWLEDGMENT

We would like to thank A. Rossi (IFAM-CNR) for target preparation and A. Barbini (IFAM-CNR) for electronic and data processing support, G. Grillon (LOA) for technical assistance during the experiments and S. Silvestri and A. Donati (ITESRE-CNR) for the invaluable help in the calibration of γ-ray detectors. We also acknowledge the scientific contribution to this work coming from the three European networks SILASI and GAUSEX and XPOSE. The experiments described in this work were also supported by the EU programme of Access to Large Scale Laser Facilities.

REFERENCES

1 T. Brabec and F. Krausz, Rev. Mod. Phys. **72**, 545 (2000) and references therein.
2 M.Nantel, J. Itatani, A. Tien, J.Faure, D.Kaplan, M.Bouvier, T. Buma et al., IEEE J. of Quant. Electr., **4**, 448 (1998).
3 L.A.Gizzi et al., Phys. Rev. E **49** 5628 (1994); M.Borghesi et al., Phys. Rev E **54,** 6769 (1996)
4 M. Galimberti, L.A.Gizzi, A.Barbini, P.Chessa, A.Giulietti, D.Giulietti, A.Rossi, Laser & Par. Beams **18**, 145 (2000),
5 L.A.Gizzi, D.Giulietti, A.Giulietti, P.Audebert, S.Bastiani, J.P.Geindre, A.Mysyrovicz, Phys. Rev. Lett. **76**, 2278 (1996).
6 D.Giulietti,L.A.Gizzi, A.Giulietti, A.Macchi, D.Teychenne , P.Chessa, A.Rousse, G.Cheriaux, J.P.Chambaret, G.Darpentigny, Phys. Rev. Lett. **79**, 3194 (1997).
7 D. Teychenne et al., Phys. Rev. E **58**, R1245 (1998).
8 A.Giulietti et al, Phys. Rev. E **59**, 1038 (1999).
9 D.Giulietti, D.Batani, V.Biancalana, A.Giulietti and L.Gizzi, Il Nuovo Cimento, 13 D, 845 (1991).
10 T.Tajima and J.M.Dawson, Phys.Rev.Lett. **43**, 267 (1979); L.M.Gorbunov and V.I.Kirsanov, Sov. Phys. JETP **66**, 290 (1987); L.Gemillet *et al*, Phys Rev. Lett., **83**, 5015(1999).
11 W.P. Leemans et al., Phys. Plasmas. **5**, 1615 (1998).
12 M.Borghesi, A.Giulietti, D.Giulietti, L.A.Gizzi, A.Macchi, O.Willi, Phys. Rev.E **54** , 6769 (1996).
13 GEANT4: LCB Status Report/RD44, CERN/LHCC-98-44, 1998
14 M. Galimberti, IFAM-REPORT, 2000.
15 M. Galimberti, A. Giulietti, D. Giulietti, L.A. Gizzi, Ph. Balcou, A. Rousse and J.Ph. Rousseau, submitted to LPB, 2001.